

Figure 23. Hydrocarbon Product Distribution and Anderson-Schulz-Flory Plot for CoB-109G; 1atm, 225 °C,  $H_2/CO = 2$ ,  $N_{\infty} = 2.66 \times 10^{-3} \text{ Sec}^{-1}$

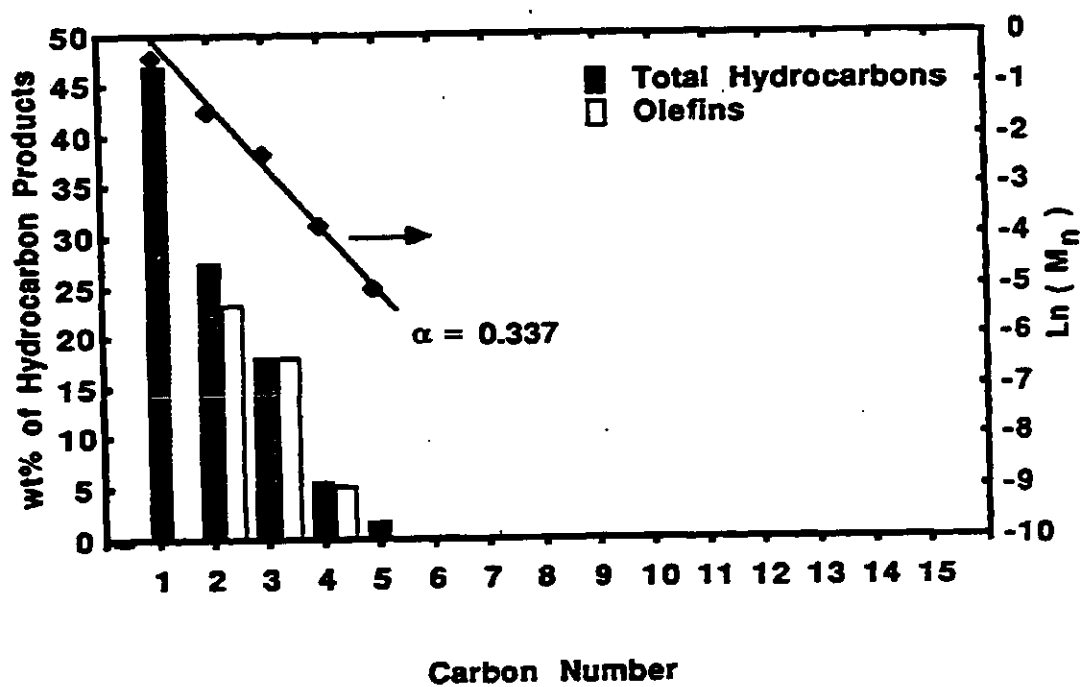


Figure 24. Hydrocarbon Product Distribution and Anderson-Schulz-Flory Plot for Co/Na; 1atm, 280 °C,  $H_2/CO = 2$ ,  $N_{\infty} = 1.35 \times 10^{-3} \text{ Sec}^{-1}$ .

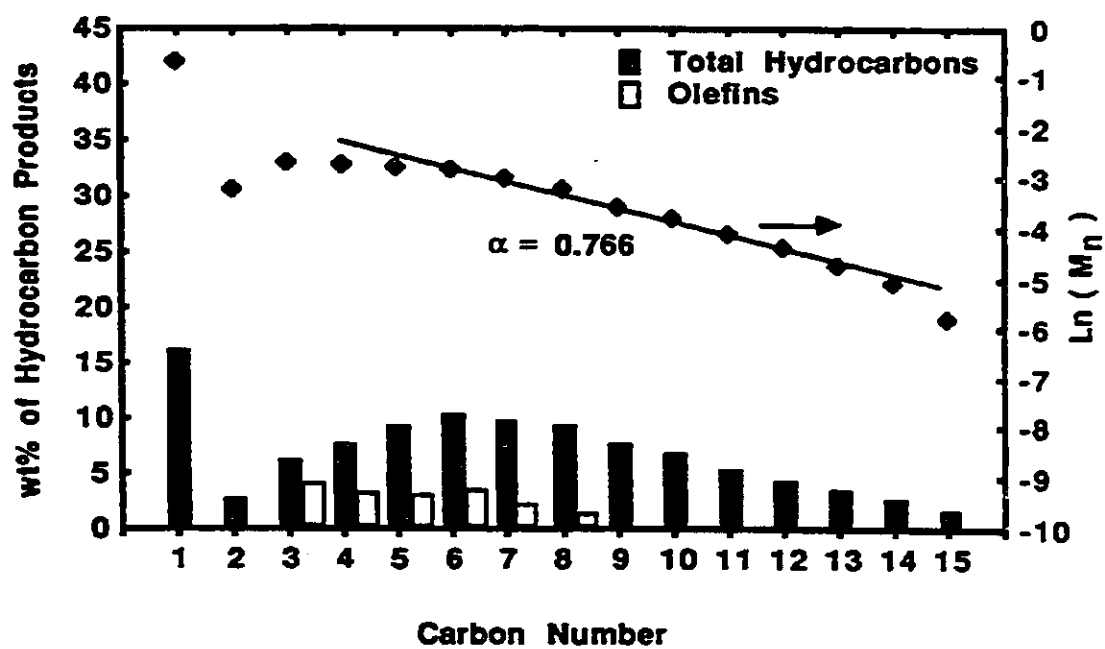


Figure 25. Hydrocarbon Product Distribution and Anderson-Schulz-Flory Plot for  $\text{CoB}/\text{Al}_2\text{O}_3$  -250; 1atm, 181 °C,  $\text{H}_2/\text{CO} = 2$ ,  $N_\infty = 7.78 \times 10^{-3} \text{ Sec}^{-1}$ .

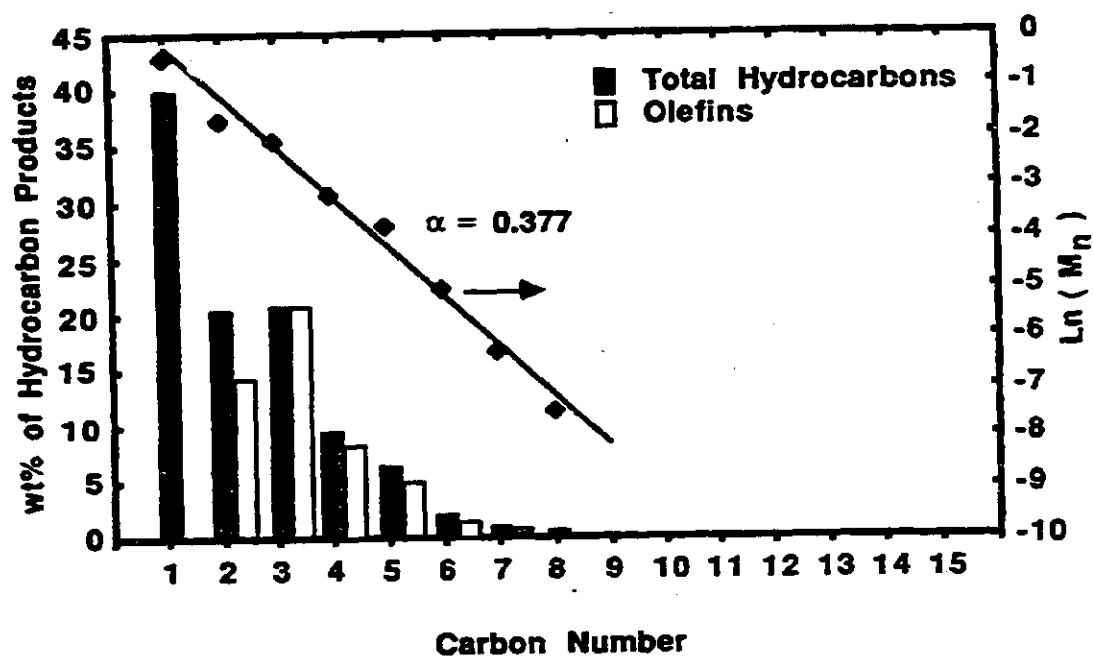


Figure 25. Hydrocarbon Product Distribution and Anderson-Schutz-Flory Plot for  $\text{CoB}/\text{Na}/\text{Al}_2\text{O}_3$  -250; 1atm, 268 °C,  $\text{H}_2/\text{CO} = 2$ ,  $N_{\text{co}} = 7.56 \times 10^3 \text{ Sec}^{-1}$ .

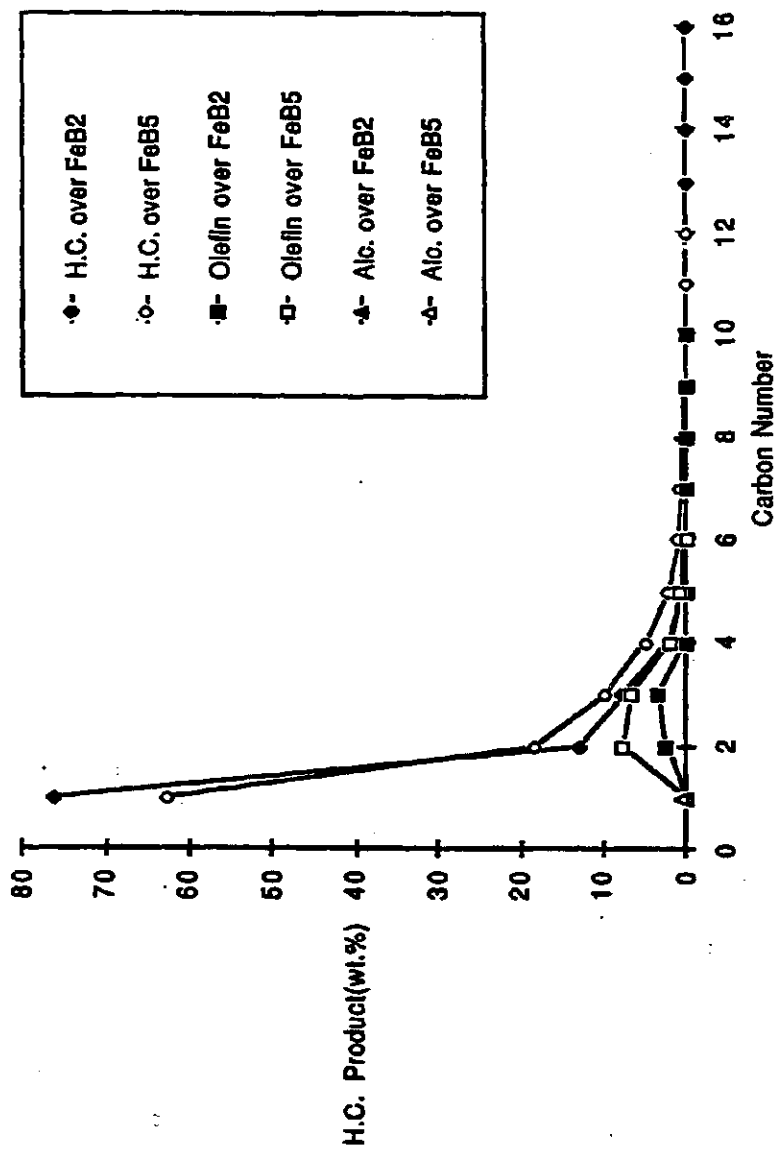


Figure 27. Hydrocarbon product distribution for H<sub>2</sub>/CO=2 reaction over FeB<sub>2</sub> at T=274 C, FeB<sub>5</sub> at 270 C, and P=21 atm.

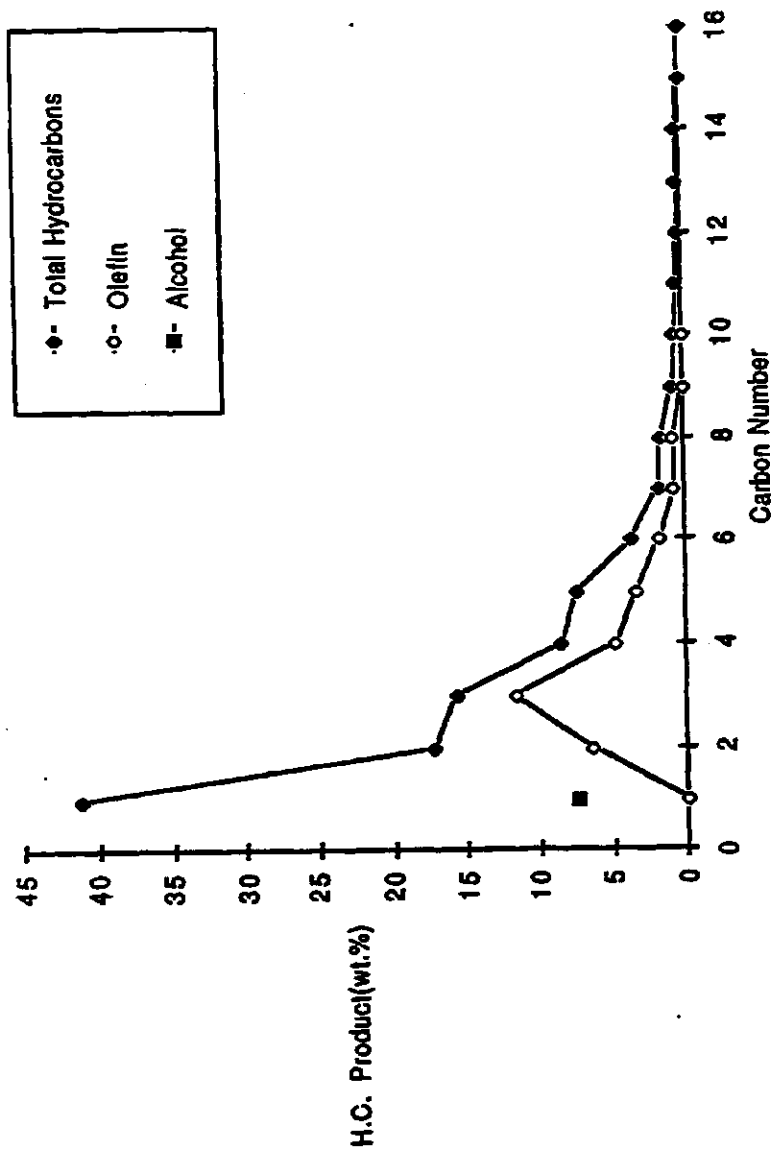


Figure 28. Hydrocarbon product distribution for Fe/B/Na at T=240 C, P=21 atm and H<sub>2</sub>/CO = 2.

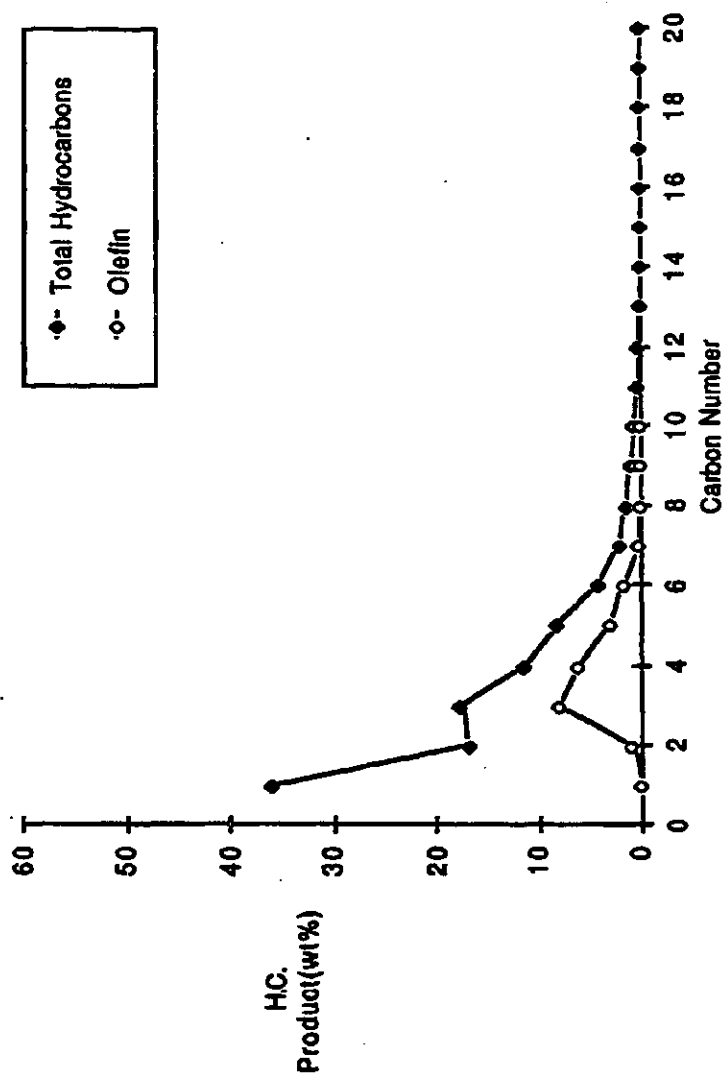


Figure 29. Hydrocarbon product distribution for FeB-COM at T=250 C, P=21 atm and H<sub>2</sub>/CO =2.

activity on the same order of magnitude as that of CoB/Al<sub>2</sub>O<sub>3</sub>-250, providing further evidence that boron causes a similar promotional effect on catalytic activity in both unsupported and supported cobalt catalysts.

CO hydrogenation activities, selectivities and activation energies of iron boride catalysts are reported in Tables 30 and 31. These catalysts were tested initially at atmosphere pressure; however, none of them possessed sufficient activity for meaningful analysis. Therefore the reactor tests were run at about 310 psia (21 atm). Only the sodium-promoted catalyst was active enough for reaction tests at 150 psia (10 atm). CO conversions were maintained below 10% by varying the space velocity at different temperatures. Since any errors in hydrogen uptake would affect the turnover frequency (TOF) calculations, mass based reaction rates (number of moles of carbon monoxide reacted per gram of catalyst per second) are also reported in these tables.

The activity of these catalysts on a turnover frequency basis increases in the order of FeB2 < FeB5 < FeB-COM < Fe/B/Na. The TOF of Fe/B/Na is about 3 times as much as that of FeB-COM while the TOF of FeB-COM is about two orders of magnitude higher than that of FeB2 or FeB5. However, the mass-based activity of FeB5 is comparable with that of FeB-COM while that of Fe/B/Na is about 20 times higher than that of FeB-COM. These differences in activity depending on basis are attributable to differences in hydrogen uptake among these catalysts.

The activity-time behavior of the iron boride catalysts varied with preparation and promoter content. For example, an increase in activity of about 200% is observed for FeB5 (at 259°C and 20 atm) during the first 20 hours and thereafter a decline of about 40% over the next 20 hours consistent with the observations of Dictor et al. [31] on reduced Fe<sub>2</sub>O<sub>3</sub>. This deactivation could be caused by reoxidation by the water product or loss of catalytic surface area during reaction. On the other hand, the activity of FeB/B/Na at 220°C and 20 atm decreased by a factor of two during the first 15 hours thereafter reaching steady state. The data in Table 31 indicate that the activity of the sodium-containing catalyst was 2 to 6 fold lower at 10 atm than at 20 atm depending on reaction temperature. The activation energy (93 KJ/mole) of the sodium free catalyst (FeB2) is slightly higher than that of 81 KJ/mole for a washed FeB prepared from NaBH<sub>4</sub> reported by Davis [32]. The unusually high E<sub>a</sub> of the commercial FeB (FeB-COM) suggests that the surface composition of this fused catalyst is different from that of the chemically reduced boride.

b. Selectivity. From the selectivity data in Table 22-29 it is evident that when compared at similar temperatures, the products obtained during CO hydrogenation over cobalt borides (CoB-250 and CoB-109G) contain larger fractions of methane and light (C<sub>2</sub>-C<sub>4</sub>) hydrocarbons and lower fractions of C<sub>5</sub>-C<sub>11</sub> and C<sub>12</sub>+ liquids relative to the products obtained over unsupported cobalt (Co-104). Accordingly the propagation probabilities (alpha values) for CoB-250 and CoB-109G are lower relative to Co-104 at any given reaction temperature. The percentage of light hydrocarbons appearing as olefins decreases in the order CoB-109G, Co-104, CoB-250. It is difficult to compare the selectivity of sodium-promoted cobalt with the other catalysts because it had to be tested at significantly higher temperatures because of its lower activity. It is clear, however, that the addition of sodium to cobalt (Table



25) increased the fraction of C<sub>2</sub>-C<sub>4</sub> olefins relative to the other catalysts. The apparent increase in olefin/paraffin ratio due to sodium is likewise evident in comparing the data for CoB-250 (Table 23) and Co8/Na-250 (Table 25). The effect of supporting cobalt boride on alumina (Table 28) is to increase its selectivity for heavier products and decrease its selectivity for olefins.

Products obtained during CO hydrogenation on iron boride catalysts (Table 30 and Figures 27-29) contain mainly methane and light hydrocarbons similar to the products observed for unpromoted iron at similar reaction temperatures [33]. Addition of sodium to iron borides (Table 31) clearly shifts selectivity in favor of lower methane production and higher olefin/paraffin ratios.

### C. Task 3: Moessbauer Spectroscopy Studies

During the first year information concerning phase changes during catalyst preparation was obtained from Moessbauer data [22-24]. For example, the Moessbauer spectrum for FeB-108 (Figure 30) prepared from aqueous phase reduction of ferric citrate when compared to spectra for fused iron borides (Table 32) provided strong evidence that Fe<sub>2</sub>B was the major catalytic phase. The room temperature spectra obtained for catalysts prepared from ethanolic reduction of ferric nitrate were not as definitive [22, 24]. Moessbauer data also provided evidence that washing of iron boride catalysts in water causes loss of boron and formation of large particles of iron oxide [22,24].

Over the past year curve fitting programs for the reduction of our Moessbauer data were obtained and modified to run on our new Sage and the University VAX computers. These programs enable us to determine line positions and intensities with high accuracy.

A new 512K 68,000 Sage II microcomputer was recently purchased and installed in our Moessbauer laboratory. It has been interfaced with our Moessbauer equipment to enable data reduction simultaneously with data collection. The Sage computer can be used for data reduction, data fitting, and data transfer to the large VAX computer.

During the second year of the contract, a liquid-nitrogen dewar was redesigned, and refitted, and tested for high vacuum operation. A Moessbauer spectrum of FeB-S-106 was characterized by a low % absorption. This was found to be due to electronic equipment problems. Efforts were made to replace the old 6800 computer with a new Radio Shack color computer with dual disk drive. The conversion turned out to be electronically quite complicated but the effort was ultimately successful.

During the 3rd and 4th years of the contract, a comprehensive Moessbauer spectroscopic investigation of iron borides was conducted to determine (1) the phases present in catalysts prepared by different techniques and (2) the phases present following FT synthesis. The results of this investigation are summarized in Table 33 and Figures 31-40.

A commercial iron boride (from Alfa Products) was analyzed by Moessbauer spectroscopy at room temperature (see Fig. 31). The spectrum before reaction (Fig. 31a) indicates that about 3% of the sample is Fe<sub>2</sub>B and 97% is FeB in

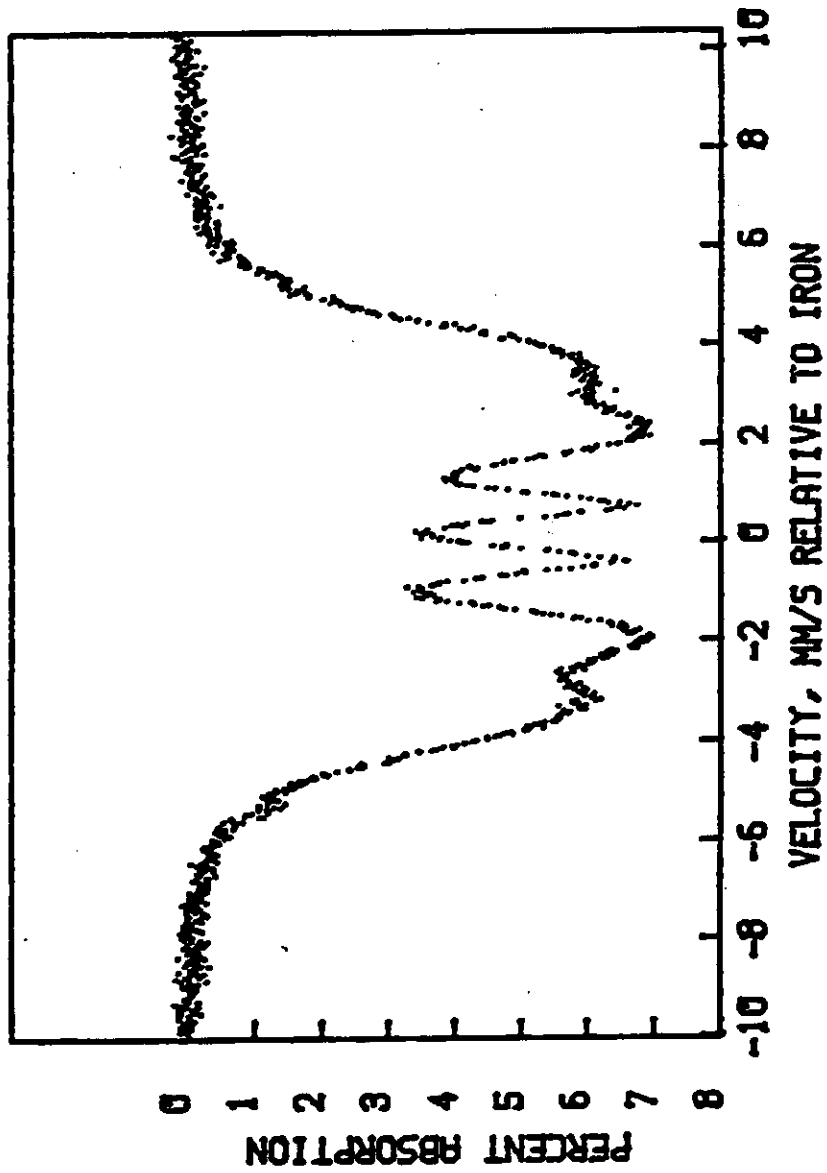


Figure 30. Moessbauer spectrum at 25° of FeB-108 after reactor testing.

Table 32. Moessbauer Parameters for Iron Borides from the literature  
(Ref. 34,35, and 36).

Species	Type of Site	Hyperfine Field(koe)	Isomer Shift mm/s(wrt Fe)	Quadropole Splitting(mm/s)	Source
FeB		$118 \pm 10$	$0.25 \pm 0.1$		Chromium
FeB		118	0.28		S. Steel
Fe <sub>2</sub> B		$240 \pm 0.1$			Chromium
Fe <sub>2</sub> B		242	0.16		S. Steel
Fe <sub>2</sub> B	Type I	$242 \pm 2$	$0.17 \pm 0.1$	$0.05 \pm 0.02$	
	Type II	$232 \pm 2$	$0.17 \pm 0.1$	$0.01 \pm 0.01$	
Fe <sub>3</sub> B	Type I	$235 \pm 5$	$0.07 \pm 0.05$	$0.024 \pm 0.05$	Copper
	Type II	$264 \pm 5$	$0.13 \pm 0.05$	$0.11 \pm 0.05$	

Table 33. Moessbauer Results for Iron Borides

Species	Species	Hyperfine Field(koe)	Isomer Shift mm/s(wrt Fe)	Quad.Splitting (mm/s)	Fraction ( % )
FeB-107-G	Fe <sup>0</sup>	333	0.016		100
FeB-COM	FeB	118	0.25		97
	Fe <sub>2</sub> B	241	0.16		3
FeB-COM- RXN	FeB	118	0.24		100
Fe(OAc) <sub>2</sub>	Fe <sup>2+</sup>		1.23	2.23	97
	Fe <sup>3+*</sup>		0.46	1.14	3
FeB2-250	Fe <sup>3+*</sup>		0.22	0.62	100
FeB2-RXN	Fe <sup>0</sup>	328	0.012		41
	Fe <sup>2+</sup>		1.17	2.42	59
FeB2-350	Fe <sup>3+*</sup>		0.24	0.65	100
FeB2-400	FeB	103	0.23		100
FeB2-460	Fe <sup>0</sup>	334	0.047		7
	FeB	102	0.24		81
	Fe <sub>2</sub> B	239	0.15		12
FeB5-250 ( LN )	Fe <sup>3+*</sup>		0.28	0.82	37
	FeB	104	0.38		63
FeB5-RXN	Fe <sup>0</sup>	332	0.008		57
	Fe <sup>2+</sup>		1.16	2.48	43
FeB5-350 ( LN )	Fe <sup>0</sup>	334	0.07		14
	Fe <sup>3+*</sup>		0.24	0.67	40
FeB5-400 ( LN )	FeB	124	0.29		46
	Fe <sup>0</sup>	336	0.1		15
	FeB	114	0.4		59
FeB5-500 ( LN )	Fe <sub>2</sub> B	242	0.13		26
	Fe <sup>0</sup>	331	0.0004		31
	FeB	112	0.31		27
Fe/B/Na NW**	Fe <sub>2</sub> B	236	0.07		42
	Fe <sup>3+*</sup>		0.20	0.64	100
Fe/B/Na** 250	Fe <sub>2</sub> B	232	0.15		100
Fe/B/Na- RXN	Fe <sup>0</sup>	333	0.02		21
	Fe <sup>2+</sup>		1.12	2.55	14
	Fe <sub>2</sub> B	236	0.14		65

\* This sharp doublet peak could be assigned to Fe<sup>3+</sup> species or fine iron boride particles

\*\* Catalyst without washing or washing with MeOH.

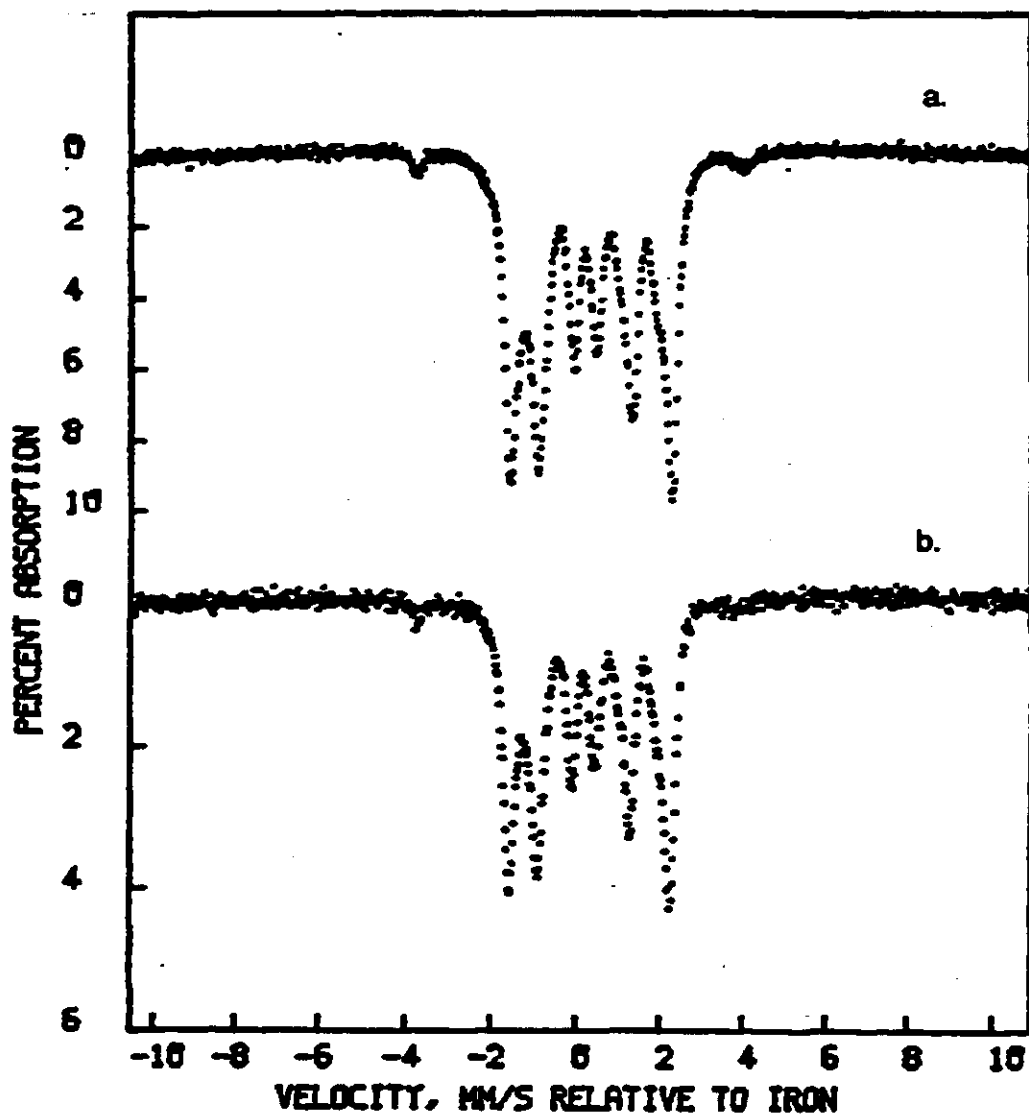


Fig. 31 Mössbauer spectra of commercial iron boride catalyst: (a) before and (b) after CO hydrogenation tests.

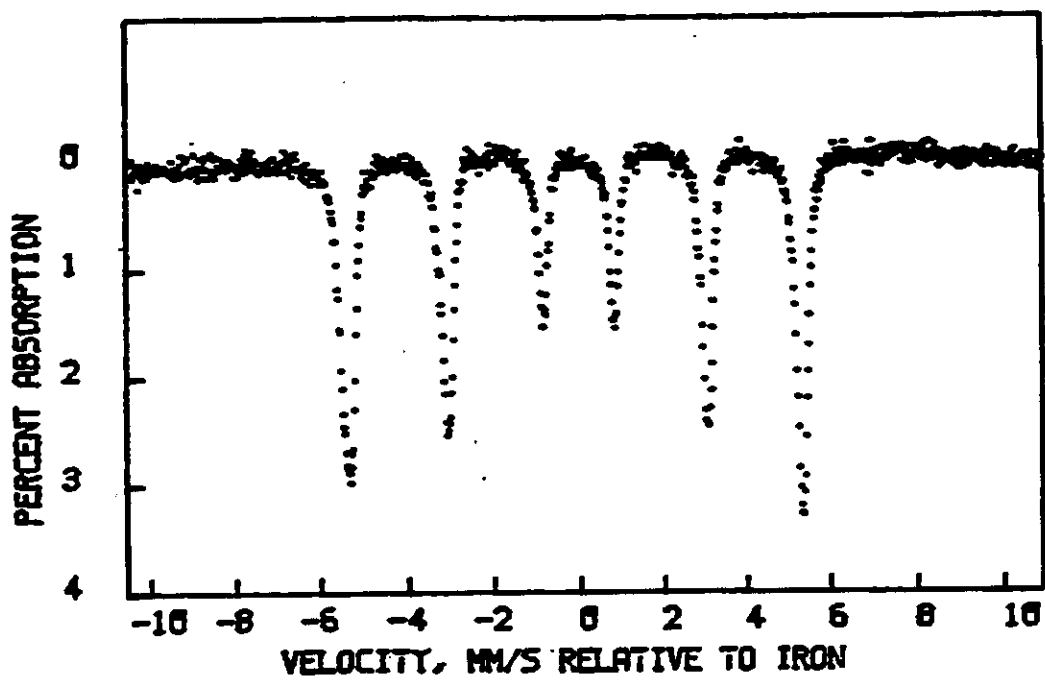


Fig. 32 Mössbauer spectrum of FeB-107-G prepared by reducing the prereduced iron oxide with a 1 %  $B_2H_6/H_2$  gas mixture at 250 °C for 1.5 hrs.

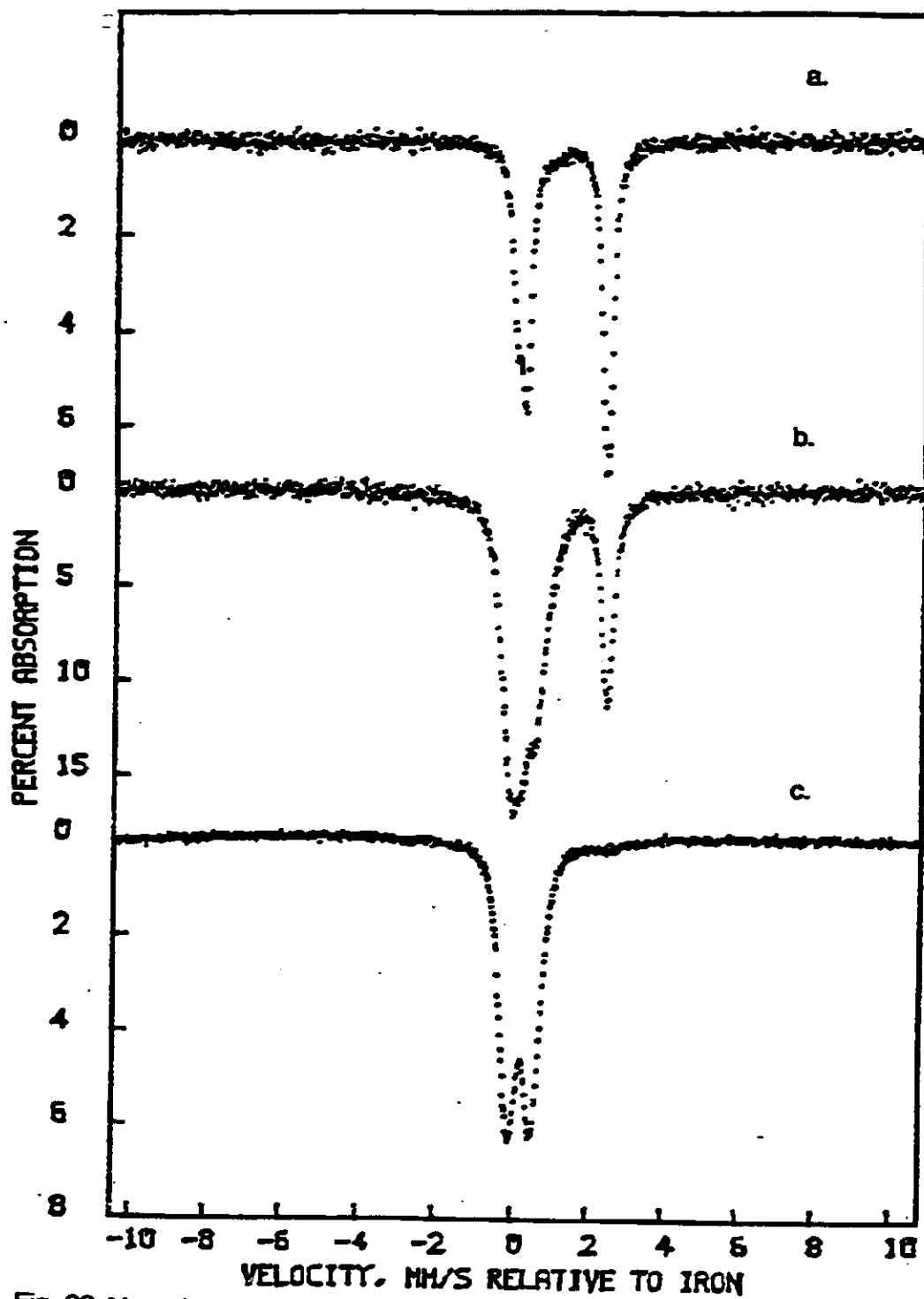


Fig. 33 Mössbauer spectra of (a) pure anhydrous iron acetate (from Alfa Products). (b) partially reduced iron acetate with  $B_2H_6/THF$ , 43 % of the iron acetate remained unreacted. (c) totally reduced iron acetate;  $FeB_2$  is produced.

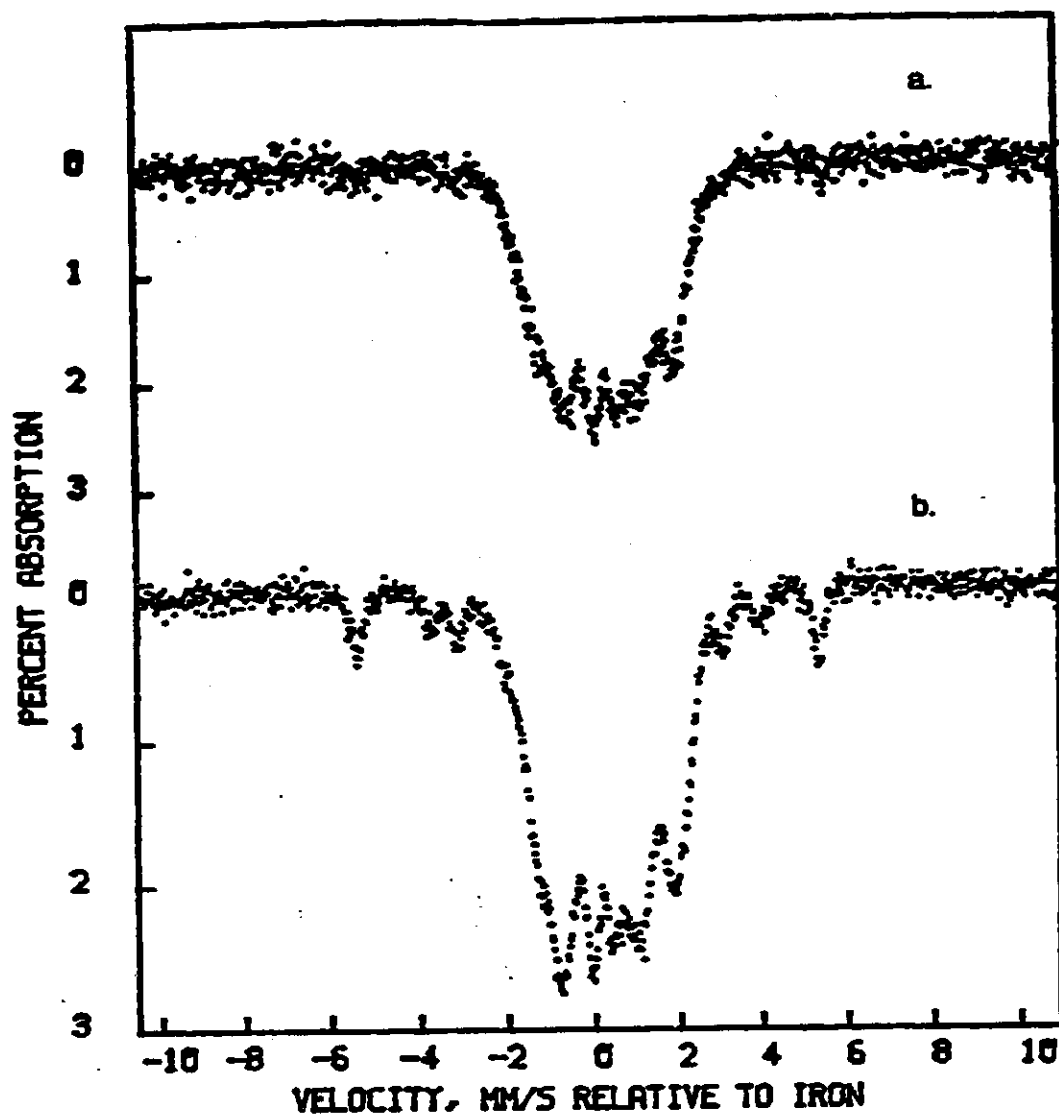


Fig. 34 Mössbauer spectra of FeB<sub>2</sub> reduced in flowing hydrogen: (a) at about 400 °C for 2 hrs. (b) reduced again at 450 °C for 18 hrs.



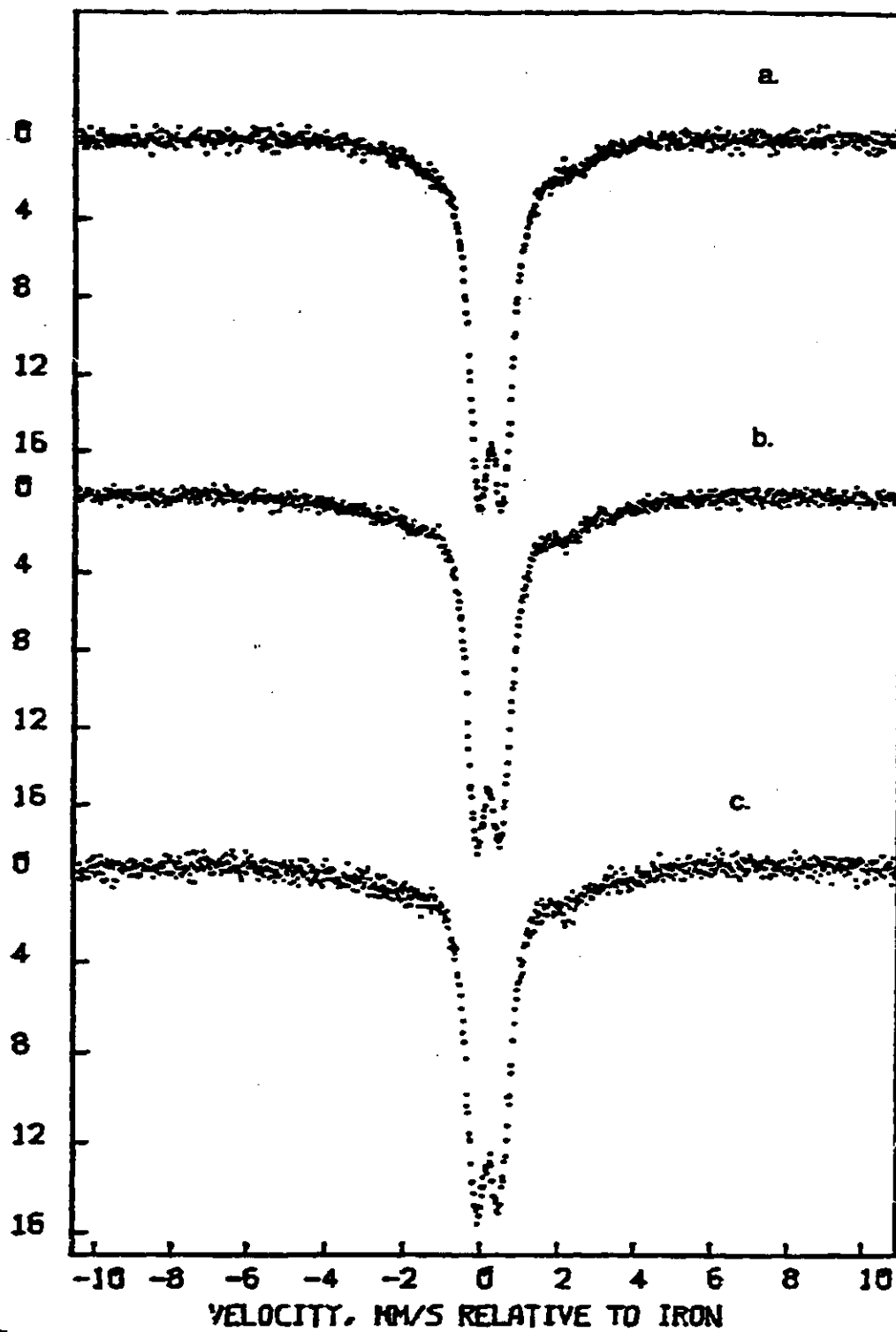


Fig. 35 In-situ Moessbauer spectra measurement on FeB5 at room temperature: (a) original sample in the cell without any treatment. (b) reduced with  $H_2$  at 250 °C for 18 hrs. (c) treated with 2:1  $H_2/CO$  mixture at 250 °C for 18 hrs.

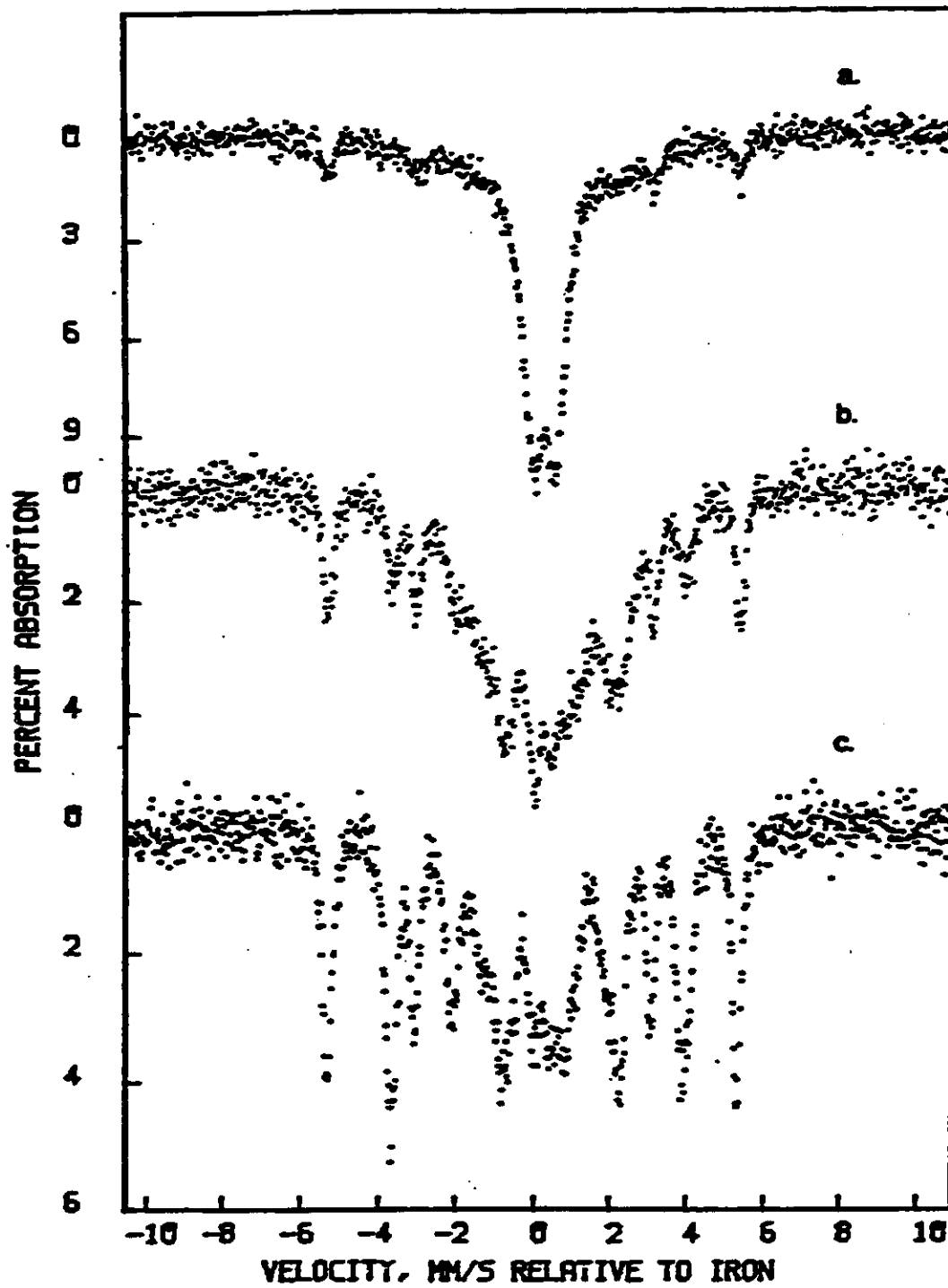


Fig. 36 Continued spectra of Fig. 7: (a) 350°C (b) 400°C, and (c) 500°C reduction with  $H_2$  for 18 hrs.

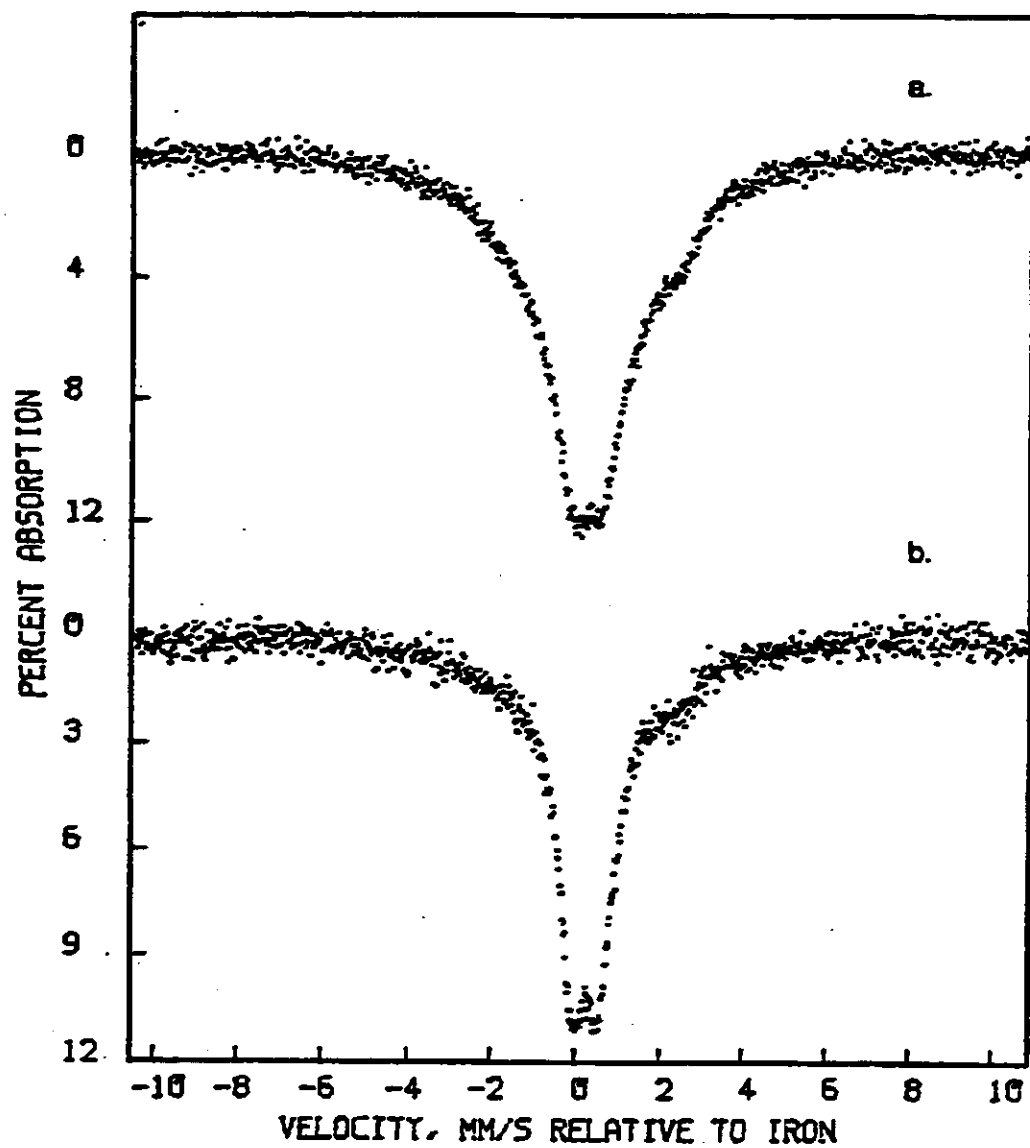


Fig. 37 In-situ Moessbauer spectra measurement of FeB5 at  $-196^{\circ}\text{C}$ : (a) after  $250^{\circ}\text{C}$  reduction with hydrogen, then (b) treated with 2:1  $\text{H}_2/\text{CO}$  mixture at  $250^{\circ}\text{C}$  for 18 hrs.

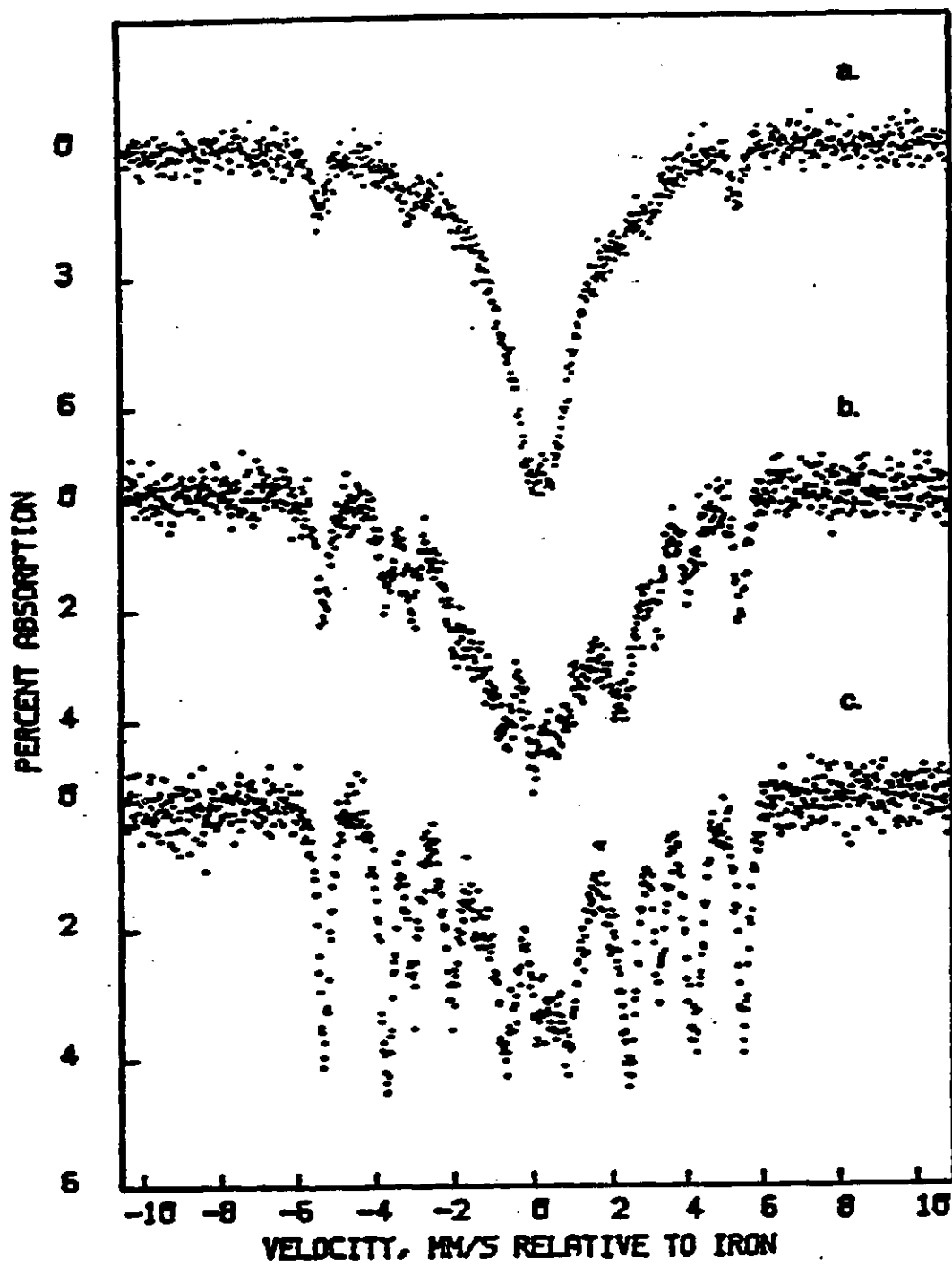


Fig. 38 Continued spectra of Fig. 9: (a) reduced again with hydrogen at 350°C (b) 400°C reduction, and (c) 500°C reduction.